This is a repository copy of *Design, control, and performance of the 'weed' 6 wheel robot in the UK MOD grand challenge*.

White Rose Research Online URL for this paper:
http://eprints.whiterose.ac.uk/90763/

Version: Accepted Version

Article:

1
2
3
4
5
6
7
8
9
10
11
12
13
14
15
16
17
18
19
20
21
22
23
24
25
26
27
28
29
30
31
32
33
34
35
36
37
38
39
40
41
42
43
44
45
46
47
48
49
50
51
52
53
54
55
56
57
58
59
60

Design, control, and performance of the 'weed' 6 wheel robot in the UK MOD grand challenge

ARJUN NAGENDRAN[1], WILLIAM CROWTHER[2], MARTIN TURNER[3],
ALEXANDER LANZON[4] and ROBERT RICHARDSON[5]

[1]Institute for Simulation and Training, University of Central Florida, USA

[2]School of Mechanical, Aerospace and Civil Engineering, University of Manchester, UK

[3] Research computing services, University of Manchester, UK

[4]School of Electrical and Electronic Engineering, University of Manchester, UK

[5]School of Mechanical Engineering, University of Leeds, UK

Abstract

A new locomotion method for unmanned (autonomous) ground vehicles (UGV) is proposed based around six independently driven wheels mounted on three separate modules. Each module is attached to the overall robot via a pivot point and capable of independently controlling its orientation and velocity. This configuration allows the UGV to perform maneuvers conventional vehicles cannot perform, and in particular to control the body orientation separately from the movement direction. The locomotion method is mathematically analyzed to develop appropriate control algorithms and to demonstrate the vehicle performance criteria. A vehicle was constructed according to the proposed configuration and experimentally tested in the UK MOD grand challenge. The performance of the developed locomotion schemes helped the robot make it to the finale of the competition.

Keywords: Autonomous Ground Vehicle, Mobile Robot Design, Robot Control, Robot Motion Analysis.

1. INTRODUCTION

This paper describes the development, design and control of an autonomous omni-directional vehicle based on independent differential-steering modules. The advantage of the vehicle lies in its mechanical simplicity i.e. no specialized mechanisms such as Mecanum wheels or Omni-directional wheels are used in the construction. It is often desirable for a small robot to carry a relatively large sensor resulting in a turret system severely compromising the performance of the robot; with this approach the sensor does not need the additional mechanical complexity and size to incorporate a turret. Moreover, driving whilst keeping the body in a constant orientation has advantages in autonomous operation, in that the sensor perspective is maintained whilst moving. As the main motors

are used to steer the robot it becomes highly maneuverable, performing steering maneuvers at relatively high speed. The information from the surveillance sensors can also be used to improve localization via Kalman filtering techniques, since the global motion of the robot and the surveillance sensor are coincident (as opposed to sensors mounted with their own actuation mechanism). The rationale behind the design allows the control algorithms to be extended to air vehicles and under-water vehicles for navigation, by treating each of the wheels as thrust vectors for its parent vehicle.

The rest of this paper is organized as follows. In Section 2, related literature in the area of wheeled locomotion is discussed. Section 3 describes the design and construction of the robot. The control strategies during different modes of operation of the robot are discussed in section 4. Section 5 presents the results of simulating complex trajectories and maneuvers for the robot. The details of the robot deployment in the UK Ministry Of Defense (MOD) Grand Challenge, including competition overview and results are discussed in Section 6, followed by conclusions in Section 7.

2.   BACKGROUND

Autonomy in mobile robots is largely determined by the locomotion method employed in the robot design.   Commonly used methods of locomotion in robots are wheels, legs, and caterpillar steering. While legs are suited to unstructured environments, permitting the robot to perform complex tasks such as climbing, they require huge computational resources for control and often involve mechanically complex design. Their speed of operation is limited on structured surfaces and they are less energy efficient in comparison to other locomotion methods under similar conditions. Skid steer systems are characterized by a larger track footprint, and hence a greater contact area, permitting them to maneuver easily across rocky or muddy terrain. It is however not possible to accurately obtain position information (odometry) to perform dead reckoning since they rely on slippage for normal operation. A large amount of energy is also lost in the form of friction between the skid steer and the surface [4]. They are also limited by the nonholonomic constraint which prevents the robot's body (center of gravity) from moving in a direction perpendicular to the direction of motion of the tracks. Wheels are a relatively simple form of locomotion for mobile robots, where the motion is described using simple mathematical models. The number of wheels, their type (fixed, active or passive) and their arrangement determines the kinematics of the underlying platform. It is generally agreed that 2 driven and steered wheels are sufficient to accomplish planar 2D motion [5]. If the center of gravity of the robot is lower than the axle attachment points, it may be sufficient to only use these 2 wheels without the need to have passive supporting wheels for stability. The robot is however susceptible to oscillations when performing certain maneuvers. A more stable configuration involves the use of a passive third wheel. Issues with kinematic compatibility such as resultant slip may be eliminated by neglecting certain control parameters; for example, in a three-wheeled robot, all compatibility

conditions are removed if two steering angles are held constant and the associated drive rates are left passive. A tricycle-drive configuration consisting of one driven front wheel and two passive rear wheels can derive odometry from a steering-angle encoder or indirectly from differential odometry [6] and is known for its inherent simplicity in control. An example is the Neptune, developed at Carnegie Melon [7], with a driven and steered front wheel and two fixed passive back wheels.

Differential drives systems offer a high maneuverability by permitting the robots to turn on the spot, with the errors in the individual wheel velocities resulting in varying trajectories and speeds. Incremental encoders can be mounted onto the drive motors to count the number of revolutions of the wheel and the equations for odometry [8, 9] can be used to compute the momentary position of the vehicle with respect to a known starting position. A simple differential drive system consists of two driven wheels with one or two passive wheels for stability. This system is again subject to the nonholonomic constraint. Another well-known steering mechanism is the Ackerman steering [10], where the inner wheel tends to be at a slightly greater angle than the outer wheel during the turn to prevent geometrically induced tire slippage. A noticeable feature of this steering mechanism is that the extended axes for all wheels intersect at a common point, meaning that each wheel follows a concentric arc about this point, with its instantaneous velocity vector being tangential to these arcs. Ackerman steering provides a fairly accurate odometry solution while supporting the traction and ground clearance needs of all-terrain operation and is therefore the method of choice for outdoor autonomous vehicles [11]. The task of controlling the robot's body in any direction in a 2D plane can be accomplished using multi-degree of freedom (MDOF) systems. Multi-degree-of-freedom (MDOF) vehicles [12] have multiple drive and steer motors and display exceptional maneuverability in tight quarters in comparison to conventional 2-DOF mobility systems [13] Several design configurations are possible. For example, HERMIES-III, an experimental test bed designed and built at the Oak Ridge National Laboratory [14, 15] has two powered wheels that are also individually steered. With four independent motors, it is a mobile robot with omnidirectional steering and is a 4-degreeof-freedom vehicle. Synchro-Drive mechanisms, which can be classified as MDOF systems, consist of three or more wheels that are mechanically coupled to rotate at the same speed and in the same direction, pivoting in unison about their own axes while executing a turn. The coupling is generally accomplished using a gear, belt or chain. Heading information is obtained through steering-angle encoder while the calculation of displacement is trivial using the encoder count and the wheel radius. A drawback with this approach is the error introduced due to compliance in drive belts, the need to control and coordinate the individual motors and the decreased lateral stability that may result from one wheel being turned in under the vehicle. To overcome this, a design (K3A) was proposed by Cybermotion that incorporates a dual-wheel arrangement on each axis [16]. The individual wheels spin in a differential configuration, with the outer wheel providing the desired stability during pivoting. However, since this is a synchro-drive mechanism, the orientation of the platform cannot be controlled, and continues to face the same direction at all times. Another

well-known multi-degree of freedom configuration is the Omni-directional configuration [17], consisting of three individually driven wheels arranged at the vertices of a triangle. By varying the angle of each wheel, it is possible to move in any direction, while also being able to turn on the spot. In more recent work, dual driven offset-caster designs for omni-directional mobility have been proposed [18], with extensions to the work handling motion in uneven terrain through the addition of suspension mechanisms [19, 20, 21]. While the design being proposed here-in is similar to the above designs, it does not employ the offset caster design. It appears that the need for the offset in the above work stems from the fact that two modules can be powered, while the third can be steered, with the offset allowing for passive steering as well as passive rotation. However, the offset means that the robot cannot configure to spin on the spot, since differential input with an offset will cause the module to drag sideways instead of rotating.

More recently, there are several researchers who have designed mechanisms that support omni-directional motion including but not limited to, Omni-Ball [22, 23], Wheel-On-Limb designs [24], Mecanum platforms [25, 26], and MY-Wheel mechanisms [27] but these do not benefit from the mechanical simplicity of having three independent differential drive modules arranged in a triangular configuration.

3. DESIGN AND CONSTRUCTION

Drawing from the advantages of the various wheel-configurations for mobile robots, a new mobile-robot wheel configuration consisting of three wheel modules was developed. Figure 1 illustrates a corner of the vehicle with the wheel module covers removed.

On each module, the bottom section contains two motors with gearboxes mounted side by side. In the centre of the module is the potentiometer that measures the module rotation with respect to the vehicle orientation. The module upper row consist of a pair of motor power electronics and in the centre a brake that allows the module angle with respect to the vehicle to be held constant (useful when going over rough terrain). Table 1 has the specifications of the components used in the design and construction of the robot.
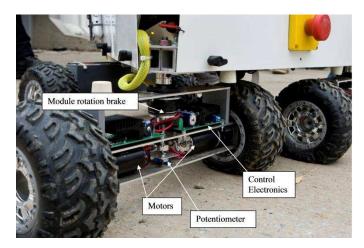
Figure 1: Close-up view of the robot wheel modules showing its components

Table 1: Specifications of the robot components

Description	NUMBER	Component
Drive motors with gearboxes	6	Maxon RE40, 150W, 24V. 15:1 gearbox
CPU	1	Gumstix controller
Sonar sensors	6	Devantech SRF02
Bullet camera	1	Sony HQ1 bullet camera
Potentiometers	3	Vishay continuous rotation
Batteries	2	Lead acid batteries
Chassis & Body work	1	Carbon fibre reinforced plastic & plastic sheet
Tyres	6	Diameter 120mm
Vehicle weight		Approximately 15kg
Size		Triangle sides 0.4m x 0.4m x0.4m
Motor controllers	6	Devantech MD03 24V, 20A H bridge motor driver.

The individual wheels of each module of the robot can be controlled, so that each wheel module is effectively a differential drive. By placing these wheel modules at the vertices of a triangle, it is possible to achieve the motion of an omni-directional robot.

Additionally, it is now possible to control the orientation of the platform independently of the direction of motion of the robot itself, thereby permitting the use of sensors such as cameras and lasers on the platform to perform sweeping motions for surveillance and mapping as the robot moves through its environment. This configuration allows the robot to achieve the motions of a tricycle-drive, synchro-drive (although modules are not directly coupled and therefore subject to greater angle error than conventional synchro-drive), and the omnidirectional steering as required. Figure 2 depicts the

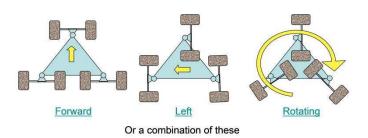robot configuration when moving forward, left and during rotation.

Figure 2: Possible motions for the 'weed' robot.

3.1. Robot sensors and navigation

One of the aims of the ground vehicle was to serve as a test-bed for the autonomy, electronics, and strategies for a hovering low flying unmanned air vehicle (UAV). This required a design that could offer multiple degrees of freedom that were illustrative of UAV maneuvers (excluding motion in the vertical plane). The proposed design allowed for testing the autonomy and electronics in a 2D plane while addressing maneuvers like strafing and spinning, and eliminating the risk involved in testing the controller on a flying vehicle. Therefore there was a size and weight limit on the sensing and computing components used. This ruled out the use of any large and heavy sensors such as 2D laser scanning and LADAR technology. A combination of a lightweight Gumstix CPU, an Inertial Measurement Unit (IMU) system by Xsens Technologies, 6 sonar sensors and a bullet camera were chosen for the task. The total mass of this system was less than 250g. Waypoints were tracked using a combination of the compass and GPS. The path-following between waypoints was implemented using a linear trajectory with parabolic blends (gradual increase in velocity to top speed, then when close to the waypoint a gradual decrease in velocity to pause at the waypoint). The sonar sensors implemented a lower level obstacle avoidance algorithm incorporating a repulsive element and random direction movement for a short fixed period of time. On encountering an obstacle the current position becomes a new way point and a new linear trajectory with parabolic blends was implemented.

4. CONFIGURATION AND CONTROL

Figure 3 shows the configuration of the robot consisting of three wheel modules that operate independently of each other and can rotate between -90^0 and $+90^0$ about their respective joint axes. The robot design is statically stable irrespective of the angular configuration of the wheel modules. The rotation of the individual wheel modules is controlled by a differential drive control scheme involving the individual pair of wheels that make up each wheel module. Each wheel module i therefore has a

velocity $V_{mod\,i}$ and an angle θ_i associated with it. These are controlled by the individual wheel velocities (V_{2i-1}, V_{2i}) which make up the wheel module i. The vector sum of the individual velocities and angles of the wheel modules gives rise to the robot's resultant vector (V, θ), along which it moves.

 Additionally, the configuration allows the orientation of the body to be independent of the direction of motion of the robot itself. i.e. the body of the robot can face a different direction to that of the robots' movement, permitting the use of a sensor such as a camera to gather information about the surroundings while constantly being on the move.
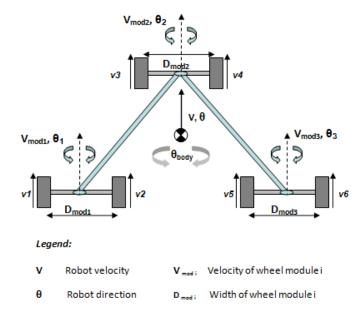

Figure 3: Robot design configuration and control parameters.

 The body angle θ_{body} is controlled by implementing a modified differential control scheme using the individual wheel velocities of the wheel modules. The different control schemes and equations for control are described in the following sections.

4.1. Orientation control of wheel modules

 The orientation of each wheel module is controlled by using differential drive that controls the angular velocity of the wheel module. If $\omega_{mod\,i}$ is the angular velocity and $D_{mod\,i}$ is the distance between the two wheels of the ith module, the following equations are valid:

$$\omega_{mod1} = \frac{v1 - v2}{D_{mod1}}, \omega_{mod2} = \frac{v3 - v4}{D_{mod2}}, \omega_{mod3} = \frac{v5 - v6}{D_{mod3}} \tag{1}$$

 A proportional controller is used to help the wheel modules achieve their desired orientation (θ_d). Potentiometers are used to obtain the current angle of each module (θ_a). The proportional gain K_p and error

$(\theta_d - \theta_a)$ determine the angular velocity $\omega_{mod\,i}$ of the wheel module i, and the individual velocities v_{2i-1} and v_{2i} of the wheels. The input to the motor controllers is calculated using (2):

$$\omega_{modi} = K_p(\theta_d - \theta_a).\omega_{modi\,max} \tag{2}$$

where $\omega_{modimax}$ is the maximum angular velocity achievable (limited by the motor characteristics). It is clear from (2) that the angular velocity applied is maximum when the error in the angle is maximum. for e.g. if the maximum velocities achievable by the individual wheels of the ith module are $v_{2i-1\,max}$ and $v_{2i\,max}$ and $K_p * (\theta_d - \theta_a)$ is scaled to be in the range 0 to 1, (2) determines the angular velocity applied to achieve the desired angle. Clearly, when $v_{2i-1\,max} = -v_{2i\,max}$, $\omega_{mod\,i}$ is maximum. The individual velocities of the wheels to achieve (2) can therefore be written as

$$v_{2i-1} = K_p * (\theta_d - \theta_a) v_{2i-1\,max} \tag{3}$$

$$v_{2i} = K_p * (\theta_d - \theta_a) v_{2i\,max} \tag{4}$$

Using equations (3) and (4), the angles of the individual wheel modules of the robot can be controlled. Depending on the response of the wheel modules to the control signal, equations (3) and (4) can be easily modified to implement a Proportional Integral Derivative (PID) or Proportional Integral (PI) controller as required.

4.2. Forward and reverse motion

The simplest form of control involves forward and reverse motion of the robot. The equations in this case are trivial, since this does not require any differential drive and the average velocity and angle of each wheel module is the same i.e.

$$v1 = v2 = v3 = v4 = v5 = v6 \tag{5}$$

$$V_{mod1} = \frac{v1 + v2}{2} = V_{mod2} = \frac{v3 + v4}{2} = V_{mod3} = \frac{v5 + v6}{2} \tag{6}$$

$$V = \frac{V_{mod1} + V_{mod2} + V_{mod3}}{3} = \frac{v1 + v2 + v3 + v4 + v5 + v6}{6} \tag{7}$$

The speed of the robot can be controlled through the use of a scaling factor $k \leq 1$. If $v_{i\,max}$ is the maximum velocity achievable by the individual wheels, $V_{i\,max} = k\,v_{i\,max}$ determines the robot's maximum velocity. To illustrate, the value of k can be 1 in the absence of any obstacles in the robot's path. A reading from an external sensor such as a sonar or laser scanner mounted on the robot can be used to re-compute the value of k in real-time, to slow the robot down as it approached an obstacle and bring it to a complete stop when within a threshold of the obstacle.

4.3. Controlling robot direction and velocity

The robot's movement is defined by its velocity V and direction of motion θ. These variables are independent of the actual orientation of the robot's body θ_{body}. It is possible for the robot to move in any direction in 2D space while keeping its body orientation a constant. This form of control requires all the wheel modules to have the same angular velocity and average linear velocity.

Let R define the distance between the Instantaneous Center of Rotation (ICR) and the robot center and vL_i and vR_i define the left and right wheel velocities of the ith module. The equations for the left and right wheels can be written as

$$vL_i = \omega_{modi}(R + \frac{D_{modi}}{2}), vR_i = \omega_{modi}(R - \frac{D_{modi}}{2}) \tag{8}$$

Since each module must have the same average linear velocity,

$$v1 + v2 = v3 + v4 = v5 + v6 = 2V \tag{9}$$

$$V_{modi} = R\omega_{modi} \tag{10}$$

Using the value of ω_{modi} from (10) in (8), the velocities of the individual wheels that make up the module can be computed. By varying the input R in (8) as a function of time i.e. R = f (t), the robot can traverse smooth trajectories such as a spline between way points.
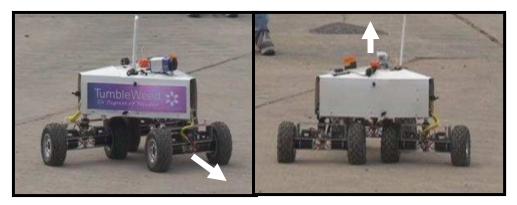

Figure 4: Constant body orientation and translation with identical linear and angular wheel velocities

4.4. Controlling robot body orientation

The unique configuration of the robot's steering permits it to have a different body angle θ_{body} as compared to the direction of its motion θ. This can be particularly useful in allowing a fixed camera mounted on the body to look in a direction that is different from the direction of motion of the robot. To implement this form of control, it is required to have different wheel module velocities, determined

by different turning radii for each wheel module. Each wheel module also has a fixed angle to maintain during the course of steering. Figure 5 illustrates the robot configuration and the radii of the wheel modules from the ICR.
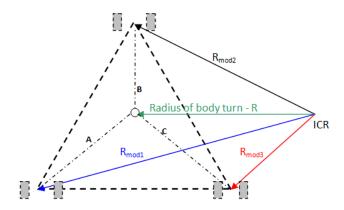

Figure 5: Illustration of robot configuration and ICR during robot steering

It can be seen that each wheel module has a different turning radius with respect to the ICR. This radius can be calculated as

$$\vec{R}_{mod1} = \vec{R} + \vec{A}$$
$$\vec{R}_{mod1} = \vec{R} + \vec{B} \tag{11}$$
$$\vec{R}_{mod3} = \vec{R} + \vec{C}$$

The angular velocity of every module is the same as the angular velocity required to rotate the body. The linear velocity however changes because of the different radii. If vL_i and vR_i define the left and right wheel velocities of the ith module, the equation for the velocities is:

$$vL_i = \omega_{modi}(R_{modi} + \frac{D_{modi}}{2}), vR_i = \omega_{modi}(R_{modi} - \frac{D_{modi}}{2}) \tag{12}$$

Note that (12) differs from (8) by virtue of the latter involving the radius of the turn from the body center, and the former involving the different radii of turn from the individual modules. Figure 6 and Figure 7 illustrate the robot in motion using this scheme. The flow control for the different schemes is shown in Figure 8 and Figure 9. The input parameters ensure that switching between the control modes has no negative effect on the performance.

Figure 6: Varying body orientation and translation direction. Every module has a constant angle, but the angles differ from one another.

Figure 7: Varying body orientation without translation by keeping wheel orientation constant – turning on the spot.
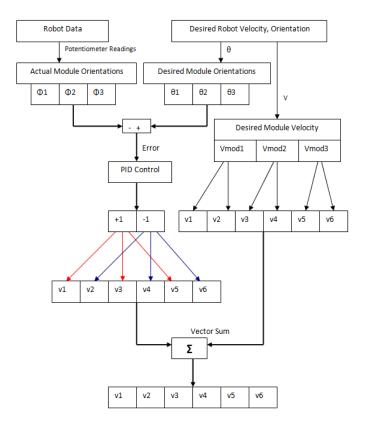

Figure 8: Combined velocity and orientation control. The desired module velocities and orientations are the same as the desired robot velocity and orientation in this configuration.
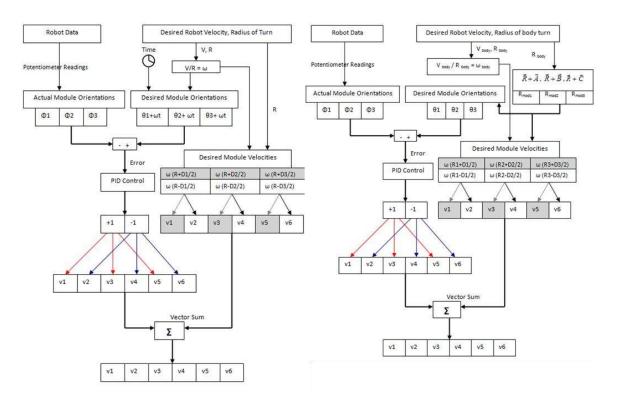
Figure 9 (a) (Left): Robot velocity control with constant body orientation. D1, D2 and D3 are the distances between the left and right wheels of modules 1, 2 and 3 respectively. Figure 10 (b) (Right): Robot velocity control with varying body orientation. D1, D2 and D3 are the distances between the left and right wheels of modules 1, 2 and 3 respectively. R1, R2 and R3 represent the radii Rmod1, Rmod2 and Rmod3 respectively.

Figures 7, 8 and 9 are provided in specific to understand the flow-control during the process and facilitate the programming of the robot's wheel modules. To help better interpret these schematics, an explanation of Figure 9 is provided here-in. The Robot Data consists of the potentiometer readings from each of the three wheel modules of the robot. This gives the orientation of each module with respect to its base frame ($\varphi 1 - \varphi 3$). The robot's global path-planner (waypoint following) requests a robot velocity $\mathbf{V_{body}}$ and a radius of turn $\mathbf{R_{body}}$ (if $\mathbf{R_{body}}$ is infinity, the robot moves in a straight line). The Radius of turn allows traversing 'splines' around obstacles rather than a 'stop-orient-move' maneuver. Figure 5 illustrates how $\mathbf{R_{body}}$ is converted to ($\mathbf{R_{mod1}} - \mathbf{R_{mod3}}$) for each module, which in turn determine their desired angles $(\theta 1 - \theta 3)$. The desired angular velocity ω is calculated as $\mathbf{V/R}$ (refer equation 10). The internal clock of the robot (microprocessor-based) is generally used along with the requested ω to compute the actual wheel module angles (as seen in figure 8), but has been omitted in figure 9. It must be noted that when constant body orientation is required (Figure 8), ω feeds into the desired module orientation, where as when the body orientation is varying, ω feeds into the desired module velocity thereby eliminating the need to compute ωt in the latter form of control. A PID controller is used to minimize the error between desired and actual orientations, with appropriate

sign conventions (+/-) used to compute the velocity for each individual wheel (6 wheels, 3 modules). The desired module velocities are calculated from which individual wheel velocities (v1 – v6) can be computed (equation (12)). A vector sum of these velocities, with the velocities from the PID control is used to determine the final velocities for each of the wheels of the three modules to perform the requested robot motion. As mentioned previously, this scheme can be extended to thruster / fans for underwater robots and air vehicles. A video demonstration of the robot using these algorithms for locomotion can be found here [28].

5.   SIMULATED TRAJECTORIES OF COMPLEX MOTION

The equations of motion developed in section 4 (equations 1 – 12) are used to simulate robot motion for different movement trajectories.

5.1. Linear robot motion with constant body rotation

This scenario involves a body movement in the y direction along the zero x-axis while the body rotates 360°. Figure 11 shows the position of the centroid and wheel modules of the robot during its motion drawn to scale. The robot spins in a clockwise direction (Z-Axis points downward according to chosen convention), as it moves forward. The linear velocity of the robot is chosen to be 1 m/s for illustration. This results in the centroid covering a distance of 5m in 5s as shown in Figure 11.
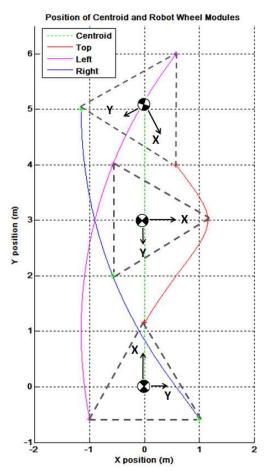
Figure 11: Linear motion with constant body rotation.

5.2. Curvilinear robot centroid motion with constant body rotation

It is possible to specify independent motions in x, y and body rotation. Here a motion is analysed where the robot body is controlled to move at a constant rate of 0.1 m/s in the X direction, a linearly increasing rate from 0 m to 0.1 m/s in the y direction and an angular rotation of 0.5235 rad/s. Figure 12 shows the position of the robot centroid and the wheel modules. The angles of the individual wheel modules and the angle of the robot body are independent of each other.

5.3. Curvilinear robot motion with body panning

In an application where sensors are rigidly aligned to the robot body, it would be useful for the body to move side to side in an oscillatory rotation; a panning motion (i.e look left, right, left…). This complex motion is achieved by combining independent robot body control and robot trajectory. The robot body orientation can be controlled as a function of time – for example, the body can exhibit sinusoidal motion to ensure a smooth, non-jerky motion during the panning, while the robot itself continues along a curvilinear path. To illustrate, the angular velocity of the body is designed to be a function of time as shown in Figure 13.
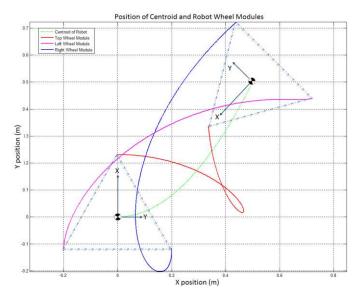
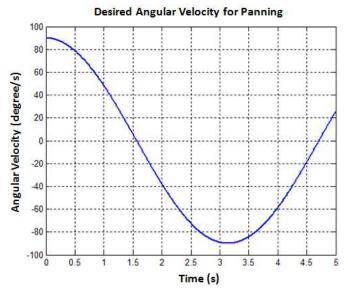Figure 12: Curvilinear robot motion with continuous body rotation.

Figure 13: Angular velocity input for panning motion.

The resulting position graph of the robot body and its wheel modules is shown in Figure 14. As illustrated, the motion of individual wheel modules becomes very complex for this motion, but it is implementable. One of the benefits of controlling the angle of individual wheel modules is that the drive motors are powerful and fast responding, allowing quick changes in module angle and velocities. One of the disadvantages of the robot design is the requirement for the wheel modules to reverse their orientation on completion of a 180^0 pivot, to prevent the electrical wiring from getting entangled. However, this can easily be overcome by using a slip ring arrangement or similar. Other disadvantages include increased control complexity, redundancy in actuators since 6 actuators are used to achieve 3

degrees of freedom. There may also be a need to lock wheels over rough terrain, since steering maybe very difficult where terrain is continuously bumpy.
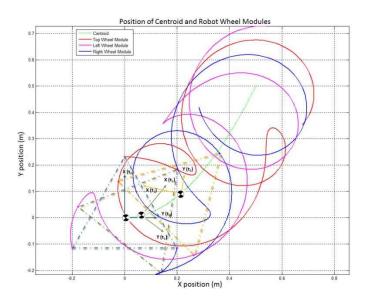

Figure 14: Curvilinear motion with body panning.

6. COMPETITION DISCUSSION AND PERFORMANCE

6.1. THE MOD GRAND CHALLENGE COMPETITION OVERVIEW

The use of autonomous robots and driverless vehicles has been the focus of several Grand Challenges including those by the UK MOD and DARPA. The first DARPA grand challenge, held in the Mojave Desert region required vehicle to autonomously complete a course of nearly 150 miles. None of the entrants were able to successfully complete this daunting task. Just a year later, during the 2005 Grand Challenge, teams had made significant progress with 5 teams completing an off-road course of 132 miles [29]. The UK ministry of defence held their first Grand Challenge with a slightly different objective:

'to deploy technological solutions to survey several square miles of hostile urban terrain to identify the location of threats.'

The competition took place in Copehill Down, a mocked-up village in the UK MOD training area, which was an unstructured environment with bushes, fences, and other assorted obstacles. Each team was allocated an hour to perform reconnaissance and identify the threats in the area. The entrants included several teams with a variety of technological solutions including a swarm of quadropters, hex-rotor UAVs, fixed-wing unmanned air vehicles, tracked-ground vehicles, and wheeled robots with differential drive capabilities.

The competition consisted of 3 qualifying events and one finale.

• Qualifying event 1:   Drive down a straight road for around ½ km and make a right turn down a side

road for another 40m.

• Qualifying event 2: Drive into an area ½ km x ½ km and automatically identify the location of a truck with a gun on the back

• Qualifying event 3: Survey an area approximately 1km x 1km and identify as many threats as possible

• Finale: Survey an area approximately 2km x 2km and identify as many threats and improvised explosive devices as possible.

A three-module differential-drive robot called 'weed' was designed and constructed as an entrant into this competition. The following sections highlight the related literature in the area, followed by detailing the robot's design, construction, configuration and control. Finally, results of field deployment are presented.

The designed vehicle was entered into the UK MOD grand challenge. Figure 15 illustrates the robot participating in the competition with the left image at a starting position and the right image showing the robot heading towards a cluttered environment.

Figure 15: The 'weed' robot competing in the UK MOD grand challenge.

Qualifying event 1 (travelling down a straight road) is fairly trivial for ground based vehicles using technologies such as laser scanners and LADAR, however it represents a significant challenge to a vehicle with sensors and computing weighing less than 250g. An important lesson to limit the number of waypoints was learnt during this mission: Around 20 waypoints were specified for this mission and at each waypoint the vehicle was programmed to perform a full 3600 visual scan – this was a very time consuming process and severely delayed the robot's progress. The transition between each waypoint was achieved by specifying a desired angular vector between points. If many waypoints are used over a short distance, then they will be close together. If waypoints are close together, then position estimate error causes large angle errors in the vehicle motion resulting in a zig-zag motion when the vehicle should be travelling in a straight line.

Qualifying event 2 required several turns on minor roads/dirt tracks that were difficult to make in an environment cluttered with trees, shrubs, telegraph poles and abandoned cars. The mission was a success and a clear image of the target vehicle was captured by the vehicle (Figure 16). A map of the

vehicle's actual trajectory, as generated and viewed by the mission planning and analysis software, developed in partnership with MBDA systems, is shown in Figure 17.

Figure 16: Target Images captured by the Robot during its mission - (left): A sniper on a building (right): A technical - target vehicle with mounted weapon.

Qualifying event 3 required a large number of complex maneuvers in a densely packed environment consisting of abandoned cars, buildings, trees, and shrubs. During this trial the vehicle encountered an abandoned car in a similar scenario to that of qualifying event 2 and the improved control strategy successfully navigated around it. However, the inability of the vehicle to look at the ground directly in front of its motion (a known limitation) resulted in the vehicle unknowingly driving off a steep bank, causing excessive vibration and disconnection of power leads. Fortunately, at this point the vehicle had demonstrated sufficient capability to qualify for the final.

For the finale, the vehicle control algorithms were set to maximum speed (until this point the control had been conservative to protect the vehicle). The route planned by the team was intended to be the most direct possible to minimize time and provide the opportunity to observe the areas most likely to contain threats. The vehicle performed well, and completed a third of the trajectory exactly as planned. However, when a third of the trajectory had been completed, an unexpected fence was encountered while driving off road between buildings. The fence completely blocked the intended route and prevented the vehicle from finishing its mission.
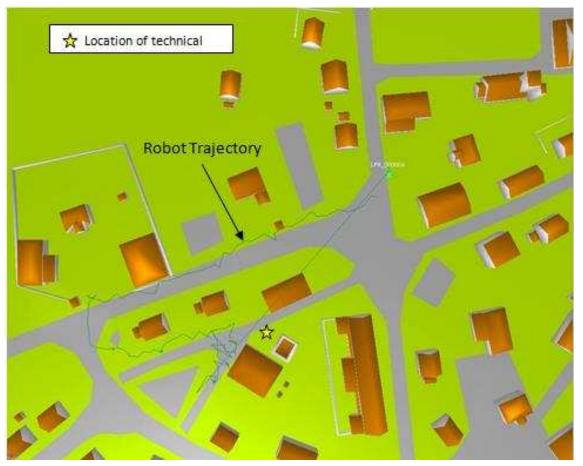
Figure 17: Mission planning and Analysis Interface.

Furthermore, it was apparent that running the motors at full speed had caused the motor drivers to overheat and it was unlikely the vehicle could have completed the course. Therefore, two lessons were learnt from this mission: i) it is important to include multiple backup mission trajectories that are activated if unexpected impassable objects are encountered. The trajectories can then be switched via a timeout if limited progress is made on the current mission trajectory. ii) Internal temperature monitoring of power electronics is crucial to ensure successful operation. Moreover, the temperature monitoring should be analogue or in many discrete steps to allow the vehicle controller to continue operation (albeit at a reduced power requirement).

7. CONCLUSION

A locomotion method based around three differentially steered modules has been proposed. Mathematical analysis of the locomotion method has proven the locomotion method feasible and algorithms have been developed to make the robot fully controllable for independent body translation and rotation. A robot has been experimentally constructed to test the locomotion method in practice and the results have demonstrated the validity of the algorithms. The robot was successfully deployed

in the UK MOD grand challenge. The design and control strategies permit mounting sensors for surveillance without the need for turret-based sensors which require additional sensors to localize them and also minimizing the number of moving-parts on a robot. Future work involves modifying the chassis to include active suspension mechanisms for mobility on uneven terrain.

ACKNOWLEDGEMENTS

REFERENCES

[1] G. Dissanayake, P. Newman, H.F. Durrant-Whyte, S. Clark, and M. Csobra, A solution to the simultaneous localisation and mapping (SLAM) problem, IEEE Transactions on Robotics and Automation, vol. 17, no. 3, pp. 229–241, 2001.

[2] C.C. Wang, C. Thorpe, and S. Thrun, On-line simultaneous localisation and mapping with detection and tracking of moving objects, in Proc. IEEE Int. Conf. Robotics and Automation, 2003, pp. 2918–2924.

[3] A.J. Davison, Y.G. Cid, and N. Kita, Real-time 3D SLAM with wide-angle vision, in Proc. IFAC/EURON Symp. Intell. Auton. Vehicles, 2004.

[4] E. U. Acar, Y. Zhang, H. Choset, M. Schervish, A. G. Costa, R. Melamud, D. C. Lean, and A. Graveline, Path Planning for Robotic Demining and Development of a Test Platform, In Proceedings of the 3rd International Conference on Field and Service Robotics (FSR), pp. 161-168, 2001.

[5] Maddocks, J. H., & Alexander, J. C. (1987). On the Kinematics and Control of Wheeled Mobile Robots: Maryland University College Park Systems Research Center.

[6] Everett, H. R. (1995). Sensors for mobile robots: theory and application: AK Peters, Ltd.

[7] Podnar, G., Dowling, D., Blackwell, M., & Carnegie-Mellon Univ Pittsburgh Pa Robotics, I. (1984). A functional vehicle for autonomous mobile robot research: Citeseer.

[8] Crowley, J. L., & Reignier, P. (1992). Asynchronous control of rotation and translation for a robot vehicle. Robotics and Autonomous Systems, 10(4), 243-251.

[9] Meng, Q., & Bischoff, R. (2005). Odometry based pose determination and errors measurement for a mobile robot with two steerable drive wheels. Journal of Intelligent and Robotic Systems, 41(4), 263-282.

[10] Byrne, R. H., Abdallah, C. T., & Dorato, P. (2002). Experimental results in robust lateral control of highway vehicles. Control Systems Magazine, IEEE, 18(2), 70-76.

[11] Borenstein, J., Everett, H. R., & Feng, L. (1996). Where am I? Sensors and methods for mobile robot positioning. Technical report, University of Michigan, 119, 120.

[12] Borenstein, J. (1995). Control and kinematic design of multi-degree-of-freedom mobile robots with compliant linkage. IEEE Transactions on Robotics and Automation, 11(1), 21-35.

[13] Abou-Samah, M., & Krovi, V. (2001). Cooperative Frameworks for Multiple Mobile Robots. In: CCTOMM Symposium on Mechanisms, Machines and Mechatronics.

[14] Pin, F. G., Beckerman, M., Spelt, P. F., Robinson, J. T., & Weisbin, C. R. (1989). Autonomous mobile robot research using the HERMIES-III robot: Oak Ridge National Lab., TN (USA).

[15] Reister, D. B. (1992). A new wheel control system for the omnidirectional HERMIES-III robot. Robotica, 10(04), 351-360.

[16] Fisher, D., Holland, J. M., & Kennedy, K. F. (1994). K3A Marks Third Generation SynchroDrive. Proc. of ANS Robotics and Remote Systems, ANS Annual Meeting, New Orleans, LA, June 19-23.

[17] Carlisle, B. (1983). An omni-directional mobile robot. Developments in Robotics, 79–87.

[18] Yu, H., Dubowsky, S., and Skwersky, A., Omni-directional Mobility Using Active Split Offset Castors. Proc of the 26th ASME Biennial Mechanisms and Robotics Conf, Sep 2000.

[19] Davis, J. J., Doebbler, J., Daugherty, K., Junkins, J. L., and Valasek, J., Aerospace Vehicle Motion Emulation Using Omni-Directional Mobile Platform, presented at the AIAA Guidance, Navigation, and Control Conference, Hilton Head, South Carolina, August 2007.

[20] Udengaard, M. and Iagnemma, K., 2008: Design of an Omnidirectional Mobile for Rough Terrain, Proc of IEEE Intl Conf on Robotics and Automation, 1666-1671.

[21] Ishigami, G., Pineda, E., Overholt, J., Hudas, G., & Iagnemma, K. (2011, September). Performance analysis and odometry improvement of an omnidirectional mobile robot for outdoor terrain. In Intelligent Robots and Systems (IROS), 2011 IEEE/RSJ International Conference on (pp. 4091-4096). IEEE.

[22] Tadakuma, K., Tadakuma, R., & Berengueres, J. (2008). Tetrahedral mobile robot with spherical omnidirectional wheel. Journal of Robotics and Mechatronics, 20(1), 125.

[23] Tadakuma, K., Tadakuma, R., & Berengeres, J. (2007, October). Development of holonomic omnidirectional Vehicle with "Omni-Ball": spherical wheels. In Intelligent Robots and Systems, 2007. IROS 2007. IEEE/RSJ International Conference on (pp. 33-39). IEE

[24] Wilcox, B. H. (2009, March). ATHLETE: A cargo and habitat transporter for the moon. In Aerospace conference, 2009 IEEE (pp. 1-7). IEEE.

[25] Salih, J. E. M., Rizon, M., Yaacob, S., Adom, A. H., & Mamat, M. R. (2006). Designing omni-directional mobile robot with mecanum wheel. American Journal of Applied Sciences, 3(5), 1831-1835.

[26] Tlale, N., & de Villiers, M. (2008, December). Kinematics and dynamics modelling of a mecanum wheeled mobile platform. In Mechatronics and Machine Vision in Practice, 2008. M2VIP 2008. 15th International Conference on (pp. 657-662). IEEE.

[27] Ye, C., & Ma, S. (2009, August). Development of an omnidirectional mobile platform. In Mechatronics and Automation, 2009. ICMA 2009. International Conference on (pp. 1111-1115). IEEE.

[28] Video demonstration of the robot maneuvers [http://youtu.be/KW-Ne540OQA]

[29] Thrun, S. (2006). Winning the darpa grand challenge. Machine Learning: ECML 2006, 4-4.